



Contents lists available at ScienceDirect

Comptes Rendus Chimie

www.sciencedirect.com



Account/Revue

# Stereochemistry of nitrogen E lone pair in $\text{NH}_3\text{E}$ , $\text{NOF}$ , $\text{N}_2\text{O}_3\text{E}_2$ , $\text{AgNO}_2\text{E}$ , and $\text{NCl}_3\text{E}$

Jean Galy<sup>a</sup>, Guillaume Couégnat<sup>a</sup>, Eladio Vila<sup>b</sup>, Samir F. Matar<sup>c,\*</sup><sup>a</sup> CNRS–LCTS, Université de Bordeaux, 33600 Pessac, France<sup>b</sup> CSIC–ICMM, Cantoblanco, 28049 Madrid, Spain<sup>c</sup> CNRS–ICMCB, Université de Bordeaux, 33600 Pessac, France

## ARTICLE INFO

## Article history:

Received 26 April 2016

Accepted 27 June 2016

Available online xxxx

## Keywords:

Electron lone pair  $\text{N}(2s^2)$ 

Crystal chemistry

DFT

ELF

## ABSTRACT

We revisit nitrogen based simple fundamental molecules in their solid state structures, with the purpose of casting new light on the stereoactivity of valence lone pairs (LPs)—formally  $\text{N}(2s^2)$ —in different crystal geometries. Based on coupled investigations of crystal chemistry and ab initio DFT calculations providing the electron localization function (ELF), LP behavior is analyzed precisely by finding its position E, orientation and “volume of influence” which consists in an electronic cloud generated around the so-called ‘centroid’ Ec of the electronic doublet. The results show the paramount importance of the role of  $\text{N}(2s^2)$  LP in the crystal network architecture through the different case studies pertaining to ammonia ( $\text{NH}_3$ ), nitrosyl fluoride (NOF), nitrosyl nitrite ( $\text{N}_2\text{O}_3$ ), silver nitrite ( $\text{AgNO}_2$ ), and nitrogen trichloride ( $\text{NCl}_3$ ). An unexpected direct ionic interaction between  $[\text{NO}]^+$  or  $\text{Ag}^+$  and the centroid Ec of the  $[\text{NO}_2\text{Ec}]^-$  nitrite group has been evidenced in  $\text{N}_2\text{O}_3\text{E}_2$  and  $\text{AgNO}_2$ , respectively.

© 2016 Académie des sciences. Published by Elsevier Masson SAS. All rights reserved.

## 1. Introduction

Several elements of the periodic table exhibit a peculiar electronic structure when they retain their last  $s^2$  electron pair, not involved in the bonding, from  $\{\text{He}\}2s^2$  up to  $\{\text{Xe}\}4f^{14}5d^{10}6s^2$  for  $\text{Po}^{4+}$ ; such elements characterized by their lone pair E  $ns^2$  ( $2 \leq n \leq 6$ ) are designated hereafter by  $\text{M}^*$ . They show generally a one sided coordination to their ligands  $2 \leq \text{CN} \leq 5$ , E completing a polyhedron which surrounds  $\text{M}^*$  up to  $\text{CN} = 6$ . In molecular chemistry, the Valence Shell Electron Pair Repulsion (VSEPR) model has been well established [1,2].

In solid state chemistry,  $\text{M}^*$  elements give a very rich family of compounds with crystal structures always revealing original characteristics with empty channels, thick layers separated by impenetrable volumes excluding any

other atoms thanks to E with its peculiar stereochemistry. In this field, for oxides, fluorides and oxyfluorides, an original approach was proposed by considering E as having a volume, non-compressible and analogous to oxygen or fluorine anions; the so-called “volume of influence” likely contributes to hcp or ccp packing [3].

A simple test was done to control the reality of E volume occupancy by calculating  $V_r$ , a reduced volume by dividing  $V$  cell volume by the  $Z$  number of O (or F) as well as E contained in the cell. As a consequence, approximate coordinates of E were obtained on the basis of the average  $\text{E}-\text{O} \sim \text{O}-\text{O}$  (or F) distance to the one sided coordinated atoms, such geometric calculation allowing to estimate  $\text{M}^*-\text{E}$  distance and direction for these  $\text{M}^* \text{E}$  units [4].

Recently, a new approach of  $\text{M}^*$  and E stereochemistry of  $6s^2$  elements by a joint crystal chemistry and ab initio analyses has been developed by two of us for  $\text{Tl}^{\text{I}}$ ,  $\text{Pb}^{\text{II}}$ ,  $\text{Bi}^{\text{III}}$  and  $\text{Po}^{\text{IV}}$ , covering all polyhedral  $\text{M}^*\text{X}_n\text{E}$  possibilities essentially for oxides, fluorides and oxyfluorides [5,6]. In

\* Corresponding author.

E-mail address: Samir.Matar@icmcb.cnrs.fr (S.F. Matar).

most of the environments except for octahedral and cubic ones, E volume departs from spherical.

The localization and size of E and its volume of influence were clearly specified. If VSEPR general rules are followed, LP–LP repulsion stronger than LP–BP, must be strictly applied in close M\* bonding because there are many examples where LP packing participates in network building by their various associations in tetrahedral chains or double layers. In these series of M\* elements, positions and sizes of E lone pairs have been defined. It was surprising but clearly established that the widest E belongs to  $\text{Ti}^+$ , its electronic doublet  $6s^2$  generating an electronic cloud (its sphere of influence) with a radius:  $r_{\text{Ti}^+} = 1.40 \text{ \AA}$ .

Our aim in this work is to focus on the nitrogen lone pair, formally  $2s^2$ , with the objective of precisely determining its location with respect to its carrier atom, i.e. its Ec centroid. We also aim at defining the LP form, size and coordinates of its volume of influence E, which is in fact the electronic cloud generated by Ec, and the final geometry of  $\text{NX}_n\text{E}$ . For this purpose, the stereochemistry of four compounds has been revisited and analyzed in the light of quantum density functional theory (DFT) [7,8] completed by fine analyses of electron localization functions (ELF) [9]:  $\text{NH}_3\text{E}$ , ammonia;  $\text{NOFe}$ , oxyfluoride;  $\text{N}_2\text{O}_3\text{E}_2$ , oxide;  $\text{AgNO}_2$ , silver nitrite and  $\text{NCl}_3\text{E}$ , nitrogen trichloride. For details on the methodology and the theory regarding DFT and ELF, the reader is kindly referred to the Annex for a brief overview and former accounts on the topic [5,6].

## 2. $\text{NH}_3\text{E}$

Ammonia is a colorless gas, lighter than air, easily solidified below 195 K.

### 2.1. Crystal structure

As shown for the first time in 1925,  $\text{NH}_3$  crystallizes in the cubic system; its unit cell contains four molecules [10]. These molecules are in a nearly perfect cubic close-packing. N atoms are located on the threefold rotation axis (4a Wyckoff site) and hydrogen atoms in 12b sites; they build typical  $\text{NH}_3$  tetrahedral isolated molecules. More recently, the refinement of the structure was published together with its electron density distribution [11]. These last crystal data are summarized in Table 1.

Based on these X-ray data, a perspective view of this molecular structure is presented in Fig. 1 in which, as a first approximation, a nitrogen lone pair E has been added to get

a general picture. Nitrogen sits on A3 threefold rotational axis and is bonded to three hydrogen atoms, being one side coordinated and making a trigonal pyramid  $\text{NH}_3$ . Owing to this symmetry, the E lone pair which, in such tetrahedral coordination, is actually an  $sp^3$  hybrid orbital, achieves a quasi-perfect model of  $\text{CN} = 3 + 1$  tetragonal geometry for  $\text{NH}_3\text{E}$ ; E was set up on A3 crystal axis using a dedicated software [12] with an approximate H–E distance of  $\sim 1.6 \text{ \AA}$ , giving  $\text{N–E} \sim 0.96 \text{ \AA}$ .

In their detailed X-ray crystal structure analyses completed by some ab initio calculations, the authors [11] have particularly emphasized the problem of N–H bending and incidentally indicated lone pair direction along A3 with  $\text{N–E} = 1 \text{ \AA}$ . E lone pair must be influential on N–H bond bending as well as on  $\angle \text{HNH}$  angle evolution even if other solutions are preferred. Nevertheless, the E stereo-structural effect is of paramount importance as shown for  $6s^2$  lone pairs replaced in their structural environment [5,6].

### 2.2. DFT and electron localization function (ELF)

Based on accurate high Brillouin zone integration, the ELF's are first used to produce the three-dimensional 3D isosurfaces shown in Fig. 2. The tetramolecular  $\text{NH}_3\text{E}$  structure is then shown with a close arrangement to that shown in Fig. 1 then the 3D ELF's in panel b) clearly highlight the E development observed on top of nitrogen.

To refine lone pair localization, precise sections through the electron localization function ELF were of paramount interest in order to define an Ec centroid position of the electron doublet on one hand, and the volume size of the electronic cloud generated by Ec centered in E on the other hand. For this purpose, electronic localization sections of  $\text{NH}_3\text{E}$ –ELF defined by (H–N–H) and (H–N–A3) planes have been realized using dedicated software built by one of us [13]. They are reported in Fig. 3. Red, green and blue areas correspond to strong, free electron gas and zero localizations, respectively. This color scheme is respected in all ELF projections.

As expected, the HNH section shows one of the faces of the  $\text{NH}_3$  trigonal pyramid with  $\text{N–H} = 1.010 \text{ \AA}$  and the  $\angle \text{HNH} = 109.8^\circ$ . Therefore, there also appears a slice of the electronic cloud E. Isodensity curves around H atom show in their center their maximum i.e. 0.99.

The following section, which contains the threefold rotation axis of the molecule, reveals precisely the lone pair:

**Table 1**  
 $\text{NH}_3\text{E}$  crystal and DFT data [11].

<b>NH<sub>3</sub>E</b> – Cubic, space group <i>P</i> 2 <sub>1</sub> 3 ( <i>N</i> <sup>o</sup> 198), <i>T</i> = 160 K									
<i>a</i> (Å)	<i>b</i> (Å)		<i>c</i> (Å)	<i>V</i> (Å <sup>3</sup> )		<i>Z</i>	<i>Vr</i> (H,E) (Å <sup>3</sup> )		
5.1305	5.1305		5.1305	135.05		4	8.4		
5.1328	5.1328		5.1328	135.23		4	8.5		
<b>Interatomic distances (Å) and angles (°)</b>									
N–H	1.010		H–H	1.646		∠HNH	109.2		
<b>Data from DFT-ELF analyses</b>									
N–H	1.030	H–H	1.662	∠HNH	107.5	N 0150Na,b,c	3.320	Ha 0150Hb,c	2.559
N–Ec	0.79	Ec–H	1.51	∠HNEc	111.4	Ec 0150Ha,b,c	1.79	H 0150Ha	2.342
N–E	0.65	E–H	1.40	∠HNE	111.4	E 0150Ha,b,c	1.87	H 0150Hb	2.758

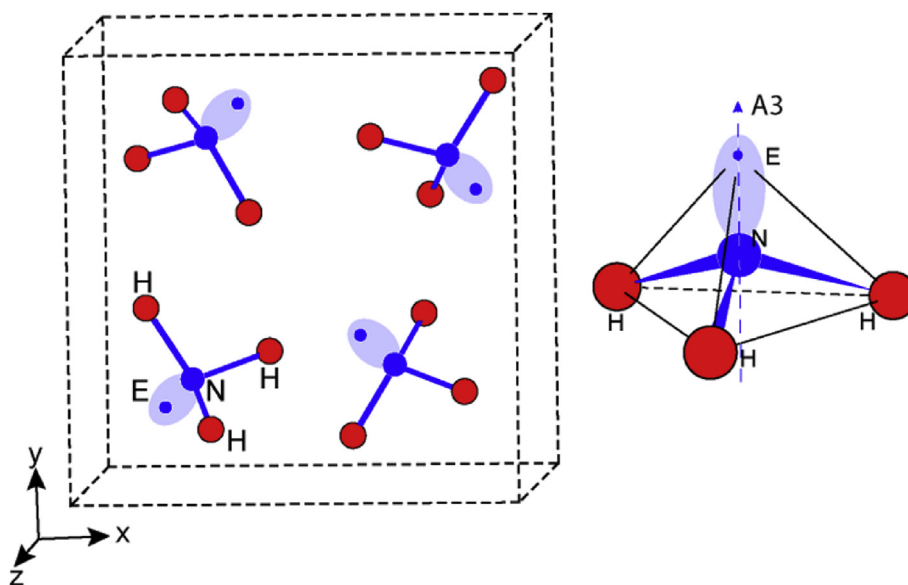


**Fig. 1.** Perspective view of the  $\text{NH}_3\text{E}$  molecular structure; E lone pair is represented schematically by an elongated ellipse whose axis indicates the N–E direction along threefold rotation axis (A3) and a blue dot indicates the center of its volume of influence. On the right hand side, the tetrahedral geometry of  $[\text{NH}_3\text{E}]$  is shown, with N atoms enclosed in a tetrahedron built by the three H atoms making an equilateral base and E situated at the apex. N and E sit on the A3 axis.

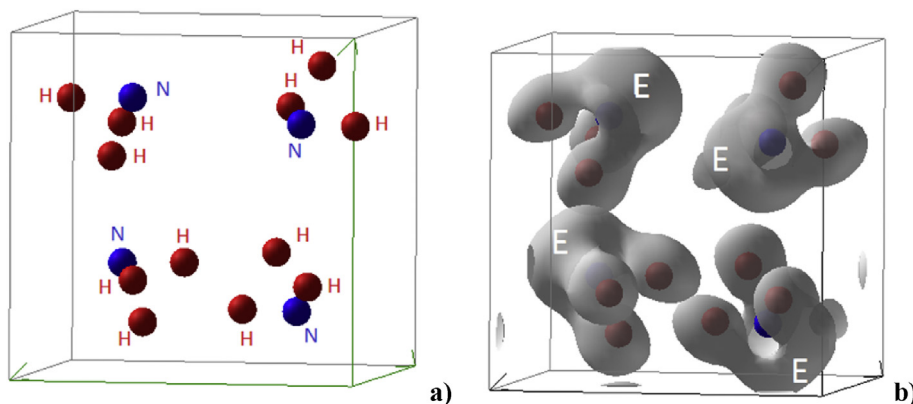


**Fig. 2.** Tetramolecular  $\text{NH}_3\text{E}$  structure from ELF calculation reproducing the schematic view in Fig. 1 (a) and the corresponding three-dimensional 3D ELF isosurfaces highlighting E volume development (b).

- the volume of E, spherical with its center onto A3 axis of course delimited in the vicinity of N atom, is roughly enclosed by the dotted blue circle with  $\phi = 1.45 \text{ \AA}$  ( $r_E = 0.73 \text{ \AA}$ ) and even appears bigger than H ions;
- E isodensity curves more spread out indicate a maximum around 0.97 which is attributed to centroid Ec (little red circle);
- like in other cases, the center of E volume (little blue circle) is somewhat displaced towards N ( $\text{Ec}-\text{E} = 0.14 \text{ \AA}$ );

Then,  $\text{NH}_3\text{E}$  shows the classical geometry where H and E define a tetrahedral geometry including N atoms as represented in (Fig. 4 left), where N and E are shown with radii,  $r_N \sim 0.38 \text{ \AA}$  and  $r_E = 0.73 \text{ \AA}$ , the hydrogen atoms being a smaller size for the sake of clear representation. This drawing shows that E sitting above the N–H bonds has an

electrostatic potential perturbing the N–H bond: i) by eventually expanding N–H by LP–BP repulsion and/or lowering the  $\angle \text{HNN}$  angle; ii) by acting simultaneously on N–H bonding electrons and H atoms therefore with different repulsive forces then bending N–H bond.

Fig. 4 (right) shows that three other  $\text{NH}_3\text{E}$  molecules surrounding each  $\text{NH}_3\text{E}$ , one hydrogen of each (Ha, Hb, and Hc) designing with the base of the former molecule, a distorted trigonal antiprism. Nitrogen and its lone pair E appear encapsulated in an H octahedron shaded in yellow in Fig. 4; pertinent distances are given in Table 1. This description is in agreement with the fact that E, the center of the electronic cloud which is largely bigger than an Ec electron doublet, is sensible to Ha,b,c repulsive effect. Consequently it is slightly pushed towards N; then a short Ec–E distance has been noticed:  $0.14 \text{ \AA}$ .

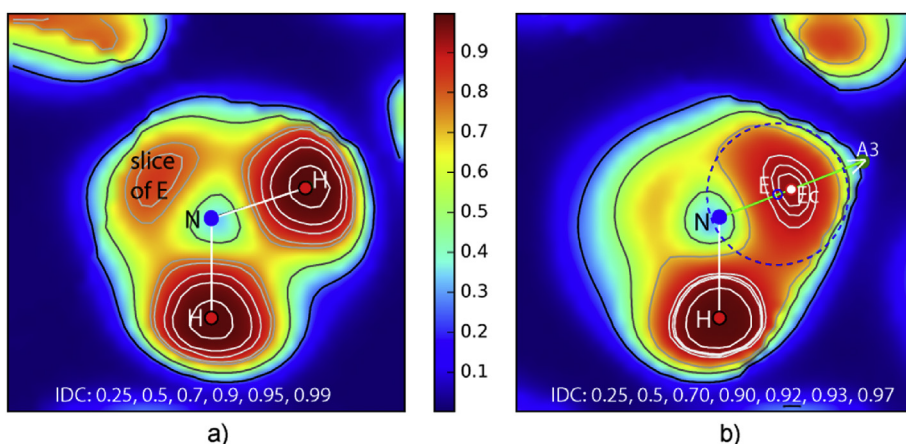


**Fig. 3.** a) Section of the DFT–ELF density by the plane (HNH), one face of the  $\text{NH}_3$  trigonal pyramid; worthy to note opposite to N–H bonds a weak density which is a slice cut in electronic cloud volume of lone pair E. The density around H atoms reaches the maximum value (0.99). b) This second section based on one H and N includes also the A3 rotation axis, showing the huge E lone pair volume. Isodensity curves permit to detect a maximum in E volume, clearly evidenced with its maximum (little red circle). The blue dotted circle delimitates lone pair electronic cloud with its E center (little blue circle).

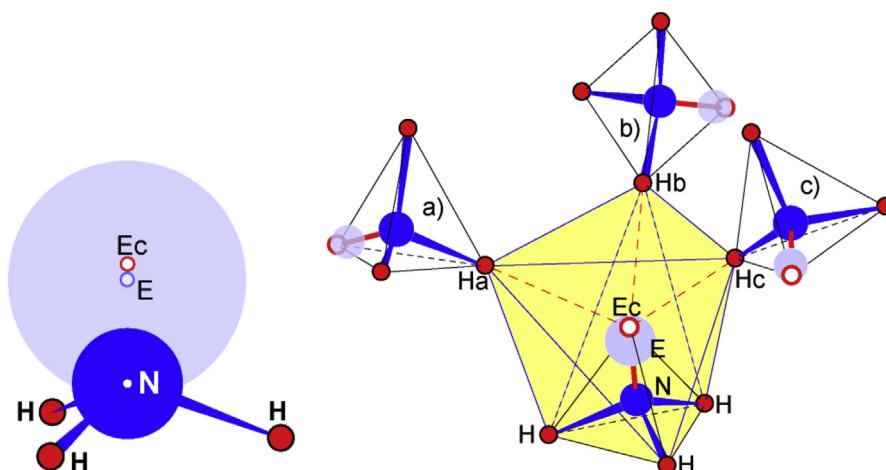


**Fig. 4.** Schematic drawing of the  $\text{NH}_3\text{E}$  molecule (left hand side) and immediate surroundings of  $\text{NH}_3\text{E}$  by three other molecules (a, b, c) making a large  $\text{N}_4$  tetrahedron (right hand side). Hydrogen atoms Ha, Hb and Hc build a distorted triangular antiprism with the ones of the base of the trigonal  $\text{MH}_3\text{E}$  (shaded in yellow) encapsulating the unit  $\text{NEEc}$ .

### 3. NOFE or $[\text{NOE}]^+\text{F}^-$ , nitrosyl fluoride

Nitrosyl fluoride was prepared by the interaction of NO with KF leading to the oxyfluoride NOF [14]. Then it was solidified below 150 K, re-crystallized and a single crystal maintained at 123 K for X-ray data collection. The NOF crystal structure belongs to an orthorhombic system. The crystallographic data are provided in Table 2.

#### 3.1. Crystal structure

Before drawing the detailed molecular packing of this oxide fluoride, an approximate position of the E lone pair associated with the nitrogen atom and its resulting shape are shown in Fig. 5 (therefore with ultimate values). The figure also shows a perspective view of the crystal network (left hand side) and the sketch of the molecular entity (right hand side).

**Table 2**  
NOFE crystal and DFT data [14].

NOFE – Orthorhombic, space group $P2_12_12_1$ ( $N^\circ 19$ ), $T = 123$ K.						
$a$ (Å)	$b$ (Å)	$c$ (Å)	$V$ (Å <sup>3</sup> )	$Z$	$V(\text{O,F,E})$ (Å <sup>3</sup> )	
4.1099	4.3910	10.202	184.11	4	15.3	
4.1838	4.4310	10.4134	193.05	4	16.1	
<i>Interatomic distances (Å) and angles (°) – crystal.</i>						
N–F	1.651	O···O in ils	3.159	$\angle$ ONF	109.7	
N–O	1.084	O···F in ils	3.308	$\angle$ ONE	134.2	
O–F	2.260			$\angle$ FNE	116.0	
N–E	0.65	E–O	1.61	E–F	2.02	
E–Fa	2.52	E–Ea,Eb	2.92	E–Fb,c	3.01	
ils: inter layer space						
<i>Data from DFT-ELF analyses</i>						
N–F	1.639	N–E	0.66	E–O	1.66	$\angle$ ONF 109
N–O	1.139	N–Ec	0.70	E–F	2.02	$\angle$ ONE 134
O–F	2.293	Ec–E	0.13	$r_E$	0.78	$\angle$ FNE 117
E ellipsoid parameters of: $a = 0.75$ Å, $b = 0.67$ Å, $c = 0.97$ Å						

The NOFE molecule is a typical triangular molecule  $M^*X_2E$  (Fig. 5 right hand side). The N–F bond is longer in  $NF_3E$  by 0.28 Å and the angle  $\angle FNO = 109.7^\circ$  is larger than  $\angle FNF = 102.2^\circ$ . Therefore, it was difficult to propose a value for the N–E distance and also for  $\angle FNE$  or  $\angle ONE$  angles. This problem is solved hereafter by DFT-ELF analyses.

The molecules packed along [100] are set up in planes parallel to (001). They delimitate two empty interlayers spaces (ils), one bordered by lone pairs (1.46 Å) centered at  $z = 0$  and  $1/2$  (shaded in pale blue color) and the second by oxygen atoms centered in  $1/4$  and  $3/4$  (2.09 Å) (pale red color). The lone pairs E directed towards blue ils planes, point to each other making a double layer of lone pairs separating NOF molecules. Interactions  $E \cdots E_{a,b}$  and  $E \cdots F_{a,b,c}$  marked by dashed red lines organize the packing of the NOFE molecules along the three directions making a double layer associated by E interactions with F and E in which NOFE molecules are packed and separated by 2.09 Å then associated by Van der Waals bonding.

### 3.2. ELF calculations

The calculated ELF at high precision is plotted in Fig. 6 along a projection close to Fig. 5 qualitative description. A slice crossing N–O–F is shown in panel a). The dominant blue zone around the NOF moiety clearly highlights the molecular character of NOF. Then within the molecule, red areas around the chemical constituents point to the electron localization and to the chemical bonding between them. Notice however the continuous red areas within NO whereas a discontinuity/separation is clearly observed between N and F. On top of N the red ELF highlights the LP. In panel b) the 3D isosurfaces are shown, highlighting further the LP (E) development. In panel c) at large isosurface values a clear observation of E (N) is exhibited spatially in the form of covering cloud.

We now turn to a more precise analysis of the ELF. Sections containing a plane with a NOF molecule and another one perpendicular to it allow appreciating the real

chemical nature of this oxide fluoride by showing clearly three zones (Fig. 7 left):

- the angular ONF geometry being drawn, a consequent cloud of electronic localization is noticed, opposed to N one sided coordination, which is of course the remarkable trace of the lone pair E completing the triangular geometry of NOFE with N found inside the OEF triangle;
- the  $N \cdots O$  bond with 1.14 Å magnitude indicates a strong bond intermediate between a triple bond (1.10 Å) a double bond (1.20 Å) and shows in its center a maximum density ( $\sim 0.80$ ) slightly blown off towards F side by E repulsive influence;
- then we note that  $N \cdots F$  line does not show any electronic concentration, indicating an  $N \cdots F$  ionic bonding with a large distance of 1.65 Å [18]. Consequently NOFE appears as an ionic molecule with a nitrosyl  $[NOE]^+$  cation and  $[F]^-$  as a counter anion.

Then it was important to analyze in detail the cloud around the lone pair to appreciate its behavior. Isodensity curves show that there is a clear maximum, which is attributed to the presence of Ec centroïd. Alike in all the previous investigations [5,6], Ec generates around it an electronic cloud, the so-called sphere of influence; its E center can be slightly displaced compared to Ec. Therefore, in such a case, there is no symmetry axis favoring spherical geometry; then E is obviously deformed, its volume been assimilated to an ellipsoid, dotted blue traces in Fig. 7 (left) from which the ellipse parameters were deduced:  $a = 0.75$  Å and  $b = 0.67$  Å in the section plane NOF and in the perpendicular plane; the third parameter  $c = 0.97$  Å Fig. 7 (right).

An average sphere of influence for E is derived with  $r_E = 0.78$  Å its center being displaced at 0.13 Å from Ec. This analysis provides also the angle values:  $\angle EcNF = 107^\circ$ ,  $\angle ENF = 117^\circ$ ,  $\angle ENO = 134^\circ$ ,  $\angle ONF = 109^\circ$ . It is worth noting how  $F^-$  anion pushes and deforms the E

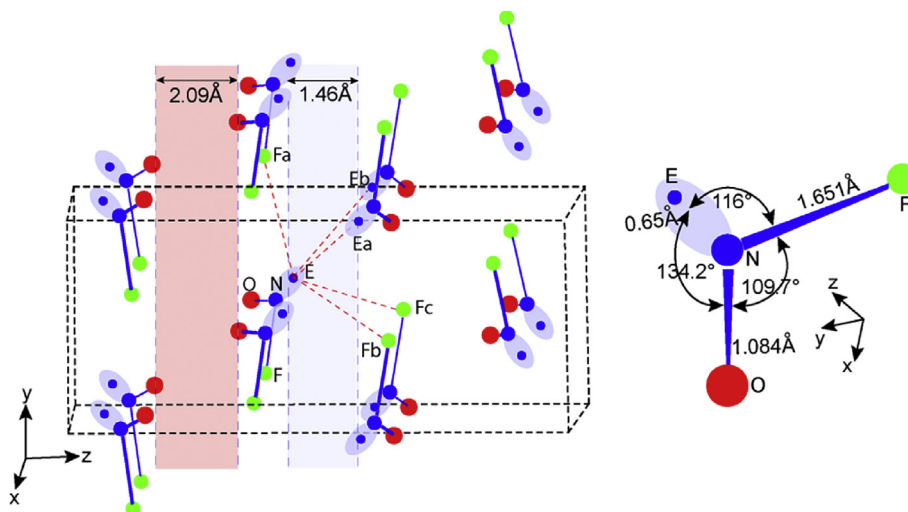
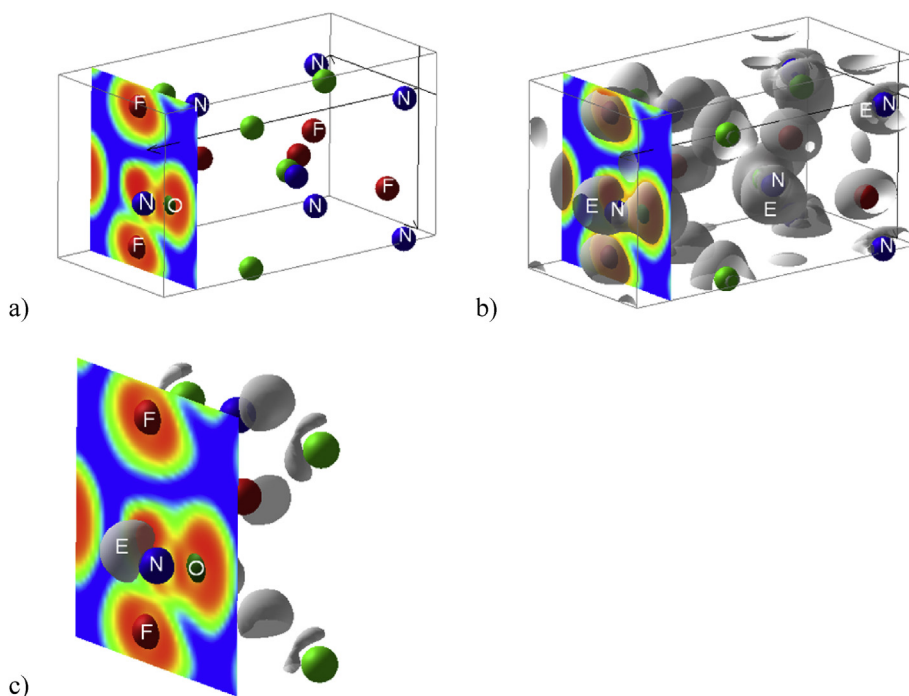
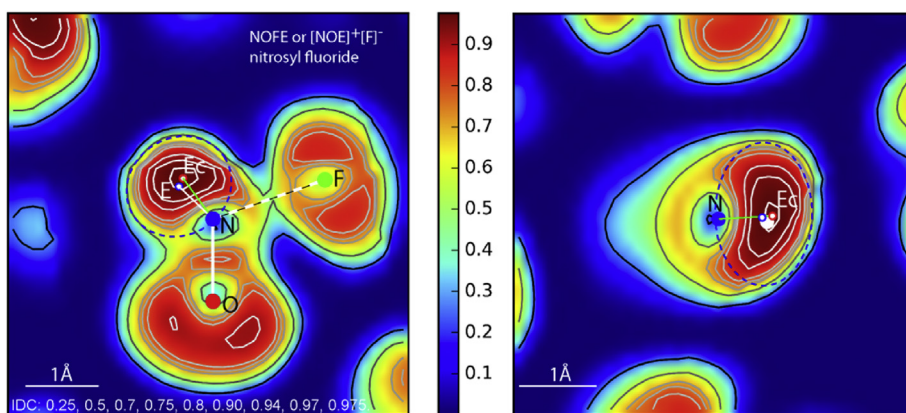


Fig. 5. Perspective view of the NOFE crystal framework and NOFE molecule.





**Fig. 6.** NOF. ELF 2D slice crossing NOF angular molecule (a) and the corresponding 3D ELF isosurfaces, highlighting the E position at N and its spatial development (b) reproducing the schematic view in Fig. 5. Panel c) illustrates further the stereospecificity of E at large isosurface values (0.89).



**Fig. 7.** ELF sections of the  $[\text{NOE}]^+[\text{F}]^-$  molecule in its plane and perpendicular aligned to N–E<sub>c</sub> (IDC: iso-density curves). Dotted blue ellipses roughly limit the ellipsoid shapes of E electronic cloud.

electronic cloud towards N=O while encountering a strong repulsive resistance which maintains high  $\angle \text{ENO} = 134^\circ$  angle. In spite of these repulsive and attractive forces, E electronic cloud, if deformed—attesting to its plasticity—is by no means broken up. Note also that its volume (radius  $r_E = 0.78 \text{ \AA}$ ) is slightly bigger than  $\text{NH}_3\text{E}$  one (radius  $r_E = 0.73 \text{ \AA}$ ).

Using this piece of information it was possible to precisely determine the direction and size of nitrogen lone pair associated with crystal network features and to calculate x, y, and z coordinates of E. Data of the  $[\text{NOE}]^+[\text{F}]^-$  molecule in the crystal structure are given in Table 2 and reported also in Fig 5 (right-hand side).

#### 4. $\text{N}_2\text{O}_3\text{E}_2$ or $[\text{NOE}]^+[\text{NO}_2\text{E}]^-$ the nitrosyl nitrite

Delicate crystal growth from the liquid around 100 K allowed obtaining single crystals suitable for X-ray analysis. At low temperatures there is a complicated phase transition system which has been described in detail [15]. Crystallographic data are summarized in Table 3.

##### 4.1. Crystal structure

Two  $\text{N}_2\text{O}_3$  varieties have been well identified, one orthorhombic B, the second tetragonal A. The former cell, orthorhombic, exhibits four independent molecules (Table

**Table 3***B* N<sub>2</sub>O<sub>3</sub>E<sub>2</sub> crystal and DFT data [15].

<b>B N<sub>2</sub>O<sub>3</sub>E<sub>2</sub></b> – Orthorhombic, space group <i>P</i> 2 <sub>1</sub> 2 <sub>1</sub> 2 <sub>1</sub> (No. 19), <i>T</i> = 113 K.							
<i>a</i> (Å)	<i>b</i> (Å)	<i>c</i> (Å)	<i>V</i> (Å <sup>3</sup> )	<i>Z</i>	<i>V</i> (O,E) (Å <sup>3</sup> )		
5.0686	6.4796	8.6326	283.52	4	14.2		
5.1763	6.6028	8.8633	302.9	4	15.1		
<hr/>							
<b>Interatomic distances (Å) and angles (°)</b>							
N1–O1	1.121	N2–O2	1.207	O2–N2–O3	128.6	N2–N1–O1	105.1
O1–O2	2.634	N2–O3	1.209	N1–N2–O2	111.9		
N1–N2	1.890	O2–O3	2.176	N1–N2–O3	119.5	∠E1N1O1	146.0
N1–E	0.64	N2–E2	0.54	N2–E2–N1	179.4	∠E1N1N2	108.7
<hr/>							
<b>Data from DFT-ELF analyses</b>							
N1–Ec1	0.67	N2–Ec2	0.58	∠O1N1N2	107.1		
N1–E1	0.57	N2–E2	0.44	∠E1N1O1	144.9		
N1–O1	1.159	N2–O2	1.227	∠E1N1N2	108.0		
N1–Ec2	1.38	N2–O3	1.225				
“N1–N2”	1.958	O2–O3	2.211	∠O2N2Ec2	111.4		
<i>r</i> <sub>E1</sub>	0.77	<i>r</i> <sub>E2</sub>	0.66	∠O3N2Ec2	119.9		
Ec1–E1	0.10	Ec2–E2	0.13				

3). A schematic drawing of the quasi planar N<sub>2</sub>O<sub>3</sub> molecule according to [15] is given in Fig. 8a. Usually it is expected to have two lone pairs one for each nitrogen, leading to N<sub>2</sub>O<sub>3</sub>E<sub>2</sub> formula the authors do not mention the lone pair existence, they nevertheless indicate the “extraordinarily long N1–N2 bond” and suggest an evolution towards a “hypothetical nitrosyl nitrite” compound.

Then a more complete shape was elaborated for the N<sub>2</sub>O<sub>3</sub>E<sub>2</sub> molecular structure as shown in Fig. 8b, based for N1 coordination on the NOE nitrosyl group well defined in NOFE (see above). For N2 it was more difficult to propose a position for E2 taking into account the established “N2–N1 bond”, so, proposals like i) E2 above and below the molecule plane (50% statistically) or ii) delocalization in a torus close to N2 having N2–N1 as an axis, were not reliable.

To clear up our view of the nitrogen lone pair problem in the N<sub>2</sub>O<sub>2</sub>E<sub>2</sub>N1OE1 molecular structure pertaining to

- their existence;
- their position;
- their volume
- and finally their outstanding role in molecular shape and crystal packing, ab initio calculations within Density Functional Theory (DFT) and Electron Localization Functions (ELF) were realized followed by precise planar sections to show via iso-density curve analyses the details of bonding scheme.

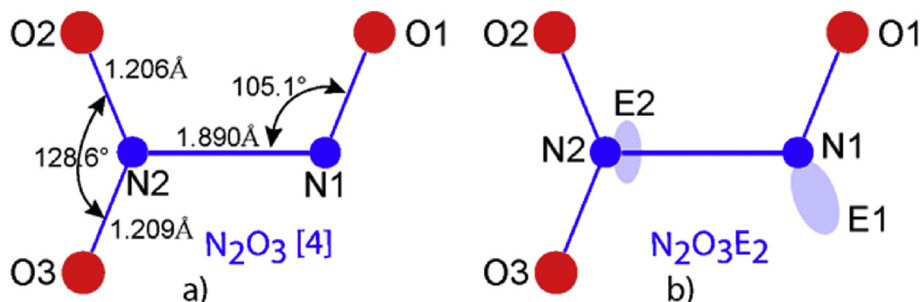
#### 4.2. ELF calculations

Fig. 9 shows the 3D ELF isosurfaces highlighting E volume development on N1 and N2 within nitrosyl NO group and nitrite NO<sub>2</sub> motifs, respectively (cf. Table 3).

Starting with the ELF full three dimensional data producing the above Fig. 9, four sections were realized. The full molecule as said above is quasi-planar as shown by both Fig. 10a and c depicted by their iso-density curves (IDCs). In the former section (Fig. 10a), the nitrite group NO<sub>2</sub> shows its two short N2–O double bonds (2.226 Å) with in their middle their trace define by an IDC around 0.75e<sup>−</sup>/Å<sup>3</sup>. But the major indication is the presence of an intense localization, opposite to the oxygen atoms O2 and O3 of nitrite group and right in the direction of N1, clearly showing the site of lone pair E2. There is a maximum density in this area which reaches 0.90e<sup>−</sup>/Å<sup>3</sup>, marked by a red circle which could be attributed to the centroid of lone pair Ec2. Then the whole volume defined by a dotted blue ellipse in this plane corresponds to the electronic cloud generated, so-called in our papers [5,6] the ‘sphere of influence’ of E the lone pair (ellipse parameters: *a* = 0.57 Å, *b* = 0.54 Å). To clarify this volume close to an ellipsoid, a section by a vertical plane passing through N2–Ec (Fig. 10b) has been drawn, giving the third parameter (*c* = 0.93 Å). Then an average spherical volume for E2 is estimated with a radius of *r*<sub>E2</sub> = 0.66 Å.

In Fig. 10a the distance N2–E2c is 0.58 Å and shows that the N2–N1 direct bond does not exist. It has been demonstrated that these lone pair electron clouds, if they are not compressible, can be deformed by various atomic interactions. In Fig. 10a, NO<sub>2</sub> nitrite group ‘wings-like’ N2–O2 and N2–O3 as well as the presence of the nitrosyl ion, are a barrier to E2 expansion itself strongly associated to its cation. Therefore these constraints leave more freedom in the vertical plane. But an electronic cloud bending towards N<sub>2</sub>O<sub>2</sub> plane is noticed. Then E2 makes a kind of electronic cap on the top of [N<sub>2</sub>O<sub>2</sub>E<sub>2</sub>]<sup>−</sup> nitrite anion (relevant data are given in Table 3).

To define E1 lone pair the ELF section by N2N1O1 plane shows a large electron cloud whose center, defined as previously, exhibits Ec1 maximum at N1–Ec1 = 0.67 Å with an IDC around 0.96e<sup>−</sup>/Å<sup>3</sup>. The E1 cloud appears somewhat distorted in its part pointing towards O3 being elongated up to the line N1–N2. Anyhow, one can admit that an ionic bond is established between N1 and Ec2.



**Fig. 8.** a) N<sub>2</sub>O<sub>3</sub> molecule scheme according to [15]; b) our starting scheme with E1 roughly alike in nitrosyl fluoride and E2 grafted onto N2.

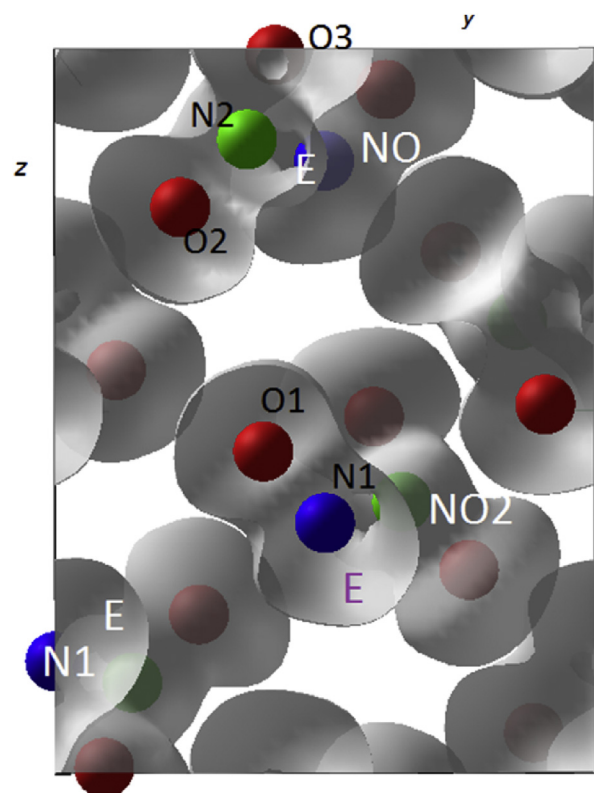


**Fig. 9.**  $\text{N}_2\text{O}_3$ : 3D ELF isosurfaces highlighting E volume development on N1 and N2 forming “NO2” and “NO” entities (cf. Table 3).

The sum of the two distances  $\text{N1-Ec2} = 1.38 \text{ \AA}$  and  $\text{Ec2-N2} = 0.58 \text{ \AA}$  amounts to  $1.96 \text{ \AA}$ , which corresponds to the “long bond  $\text{N2-N1} = 1.958 \text{ \AA}$ ”.

Then the nitrosyl group  $[\text{NOE}]^+$  is now well defined (data in Table 3) and  $\text{N}_2\text{O}_3\text{E}_2$  appears as a real nitrosyl nitrite  $[\text{NOE}]^+[\text{NO}_2\text{E}]^-$  entity which is represented in Fig. 11b and also in its molecular crystal network (Fig. 11a).

## 5. Comparison with $\text{N}_2\text{O}_4$ and NOFE

The nitrosyl nitrite molecule, like  $\text{N}_2\text{O}_4$ , is quasi planar (small torsion angle  $\sim 3.2^\circ$  between the two angular and triangular groups) – Fig. 12, therefore by comparison some remarkable differences must be noted showing an E stereochemical role. In  $\text{N}_2\text{O}_3\text{E}_2$  molecule  $\text{N2-O2}$  and  $\text{N2-O3}$  bonds are slightly longer, around  $0.03 \text{ \AA}$ , but the  $\angle \text{O2N2O3}$  angle is pinched evolving from  $134.3^\circ$  to  $128.6^\circ$ , an effect directly linked to LP–BP repulsion exerted by Ec2 on N–O bonding. Note also that the  $\text{N2-Ec2-N1}$  long interatomic distance, partly ionic ( $\text{N1-Ec2}$ ), is enlarged up to  $1.890 \text{ \AA}$  compared to the real bond  $\text{N-N}' = 1.758 \text{ \AA}$  in  $\text{N}_2\text{O}_4$  [16].

Interesting also to compare the NOE nitrosyl part of  $\text{N}_2\text{O}_3\text{E}_2$  with the one of NOFE (Fig. 12) both exhibiting typical angular geometry.  $\text{N1-E1}$  and  $\text{N-E}$  show the same value of  $\sim 0.68 \text{ \AA}$  but if  $\text{N1-O1} = 1.159 \text{ \AA}$  indicating a double bond character in NOFE,  $\text{N-O} = 1.084 \text{ \AA}$  tends to a triple bond. The ionic bonding  $\text{N1-Ec2} = 1.38 \text{ \AA}$  is markedly shorter than  $\text{N-F} = 1.651 \text{ \AA}$ , inducing an

inverted conclusion when  $\angle \text{ENO}$  angle is considered:  $144.9^\circ$  for N1 and  $134^\circ$  for N. This lets suggest that the repulsion of  $\text{F}^-$  anion bigger than the concentrated Ec2 has a more effective impact attached to its size on O and E in spite of being at a larger distance. The same effect touches the  $\angle \text{ENF}$  and  $\angle \text{ONF}$  angles considerably enlarged in NOFE (Fig. 12).

## Note

It is important to underline for this molecule the phase transition giving at higher temperature a new polymorphic phase  $\text{A-N}_2\text{O}_3\text{E}_2$  crystallizing in tetragonal system space group  $I4_1/a$  with  $a = b = 16.2557 \text{ \AA}$ ,  $c = 8.8049 \text{ \AA}$ , and  $Z = 32$ ). This large cell exhibits two independent  $\text{N}_2\text{O}_3\text{E}_2$  molecules in asymmetric units, A and B, this last unit showing two conformations B1 and B1'. These molecules are very similar to the one in  $\text{B-N}_2\text{O}_3\text{E}_2$  form with their  $[\text{NO}_2\text{E}]^-$  nitrite ion, the nitrosyl group  $[\text{NOE}]^+$  in the B unit flipping between two positions (50% occupancy). The fact that these three forms of  $\text{N}_2\text{O}_3\text{E}_2$  molecules show similar crystallographic parameters (bonds and angles) testifies that the ionic interaction  $\text{N1-Ec2}$  underlined above linking up nitrite  $[\text{N}_2\text{O}_2\text{E}]^-$  and nitrosyl  $[\text{N1OE}]^+$  group is well established supporting phase transition with a full molecule dispatching in various positions.

This  $\text{N1-Ec}$  ionic bonding appears rather unusual because the electronic doublet  $2s^2$  plays the role of an anion like a fluoride for example, well illustrated by  $[\text{NOE}]^+\text{F}^-$  here above.

To verify if such a possibility exists under other conditions, we have analyzed silver nitrite  $\text{AgNO}_2\text{E}$  crystal structure and calculated its ELF.

## 6. Comparison of silver nitrite $\text{AgNO}_2\text{E}$ with $[\text{N}_2\text{O}_2\text{E}]^-$ $[\text{N1OE}]^+$

$\text{AgNO}_2\text{E}$  crystallizes in the orthorhombic system [17]. The data are reported in Table 4.

A view of the crystal network is given in Fig. 13. Six nitrite groups  $\text{NO}_2\text{E}$  all parallel to the (100) plane are distributed at the apices of an octahedron encapsulating the silver atom. In the equatorial plane four oxygen atoms of four different  $\text{NO}_2$  groups form the rectangular base of a large square prism on the top of which sit Oe and Of of the  $\text{NcO}_2\text{E}$  group. Finally there is an oxygenated hexahedron surrounding Ag with relatively large Ag–O interatomic distances. It is worthy noting that in the [001] direction there is a sixth  $\text{NO}_2\text{E}$  group showing an Ag–N distance of  $2.471 \text{ \AA}$  therefore including in between the E lone pair; then deducing that the sixth nitrite group should be linked to Ag by ionic bonding Ag–E.

Consequently calculations were of paramount importance to establish this sequence  $\text{N-E-Ag}$  by comparison with  $\text{N2-Ec2-N1}$  found in  $\text{N}_2\text{O}_3\text{E}_2$ . The DFT and ELF resulting data are given in Table 4.

Fig. 14 shows the extended cell of  $\text{AgNO}_2$  with grey 3D ELF isosurfaces around  $\text{NO}_2^-$  nitrite entities, around electropositive Ag like an alkaline cation characterized by the absence of electron localization (no isosurface). Note the close relationship with the schematic view in Fig. 13.

Two sections were done in the three dimensional ELF, one following the plane formed by N, O and Ag atoms which shows the presence of E, the second perpendicular,



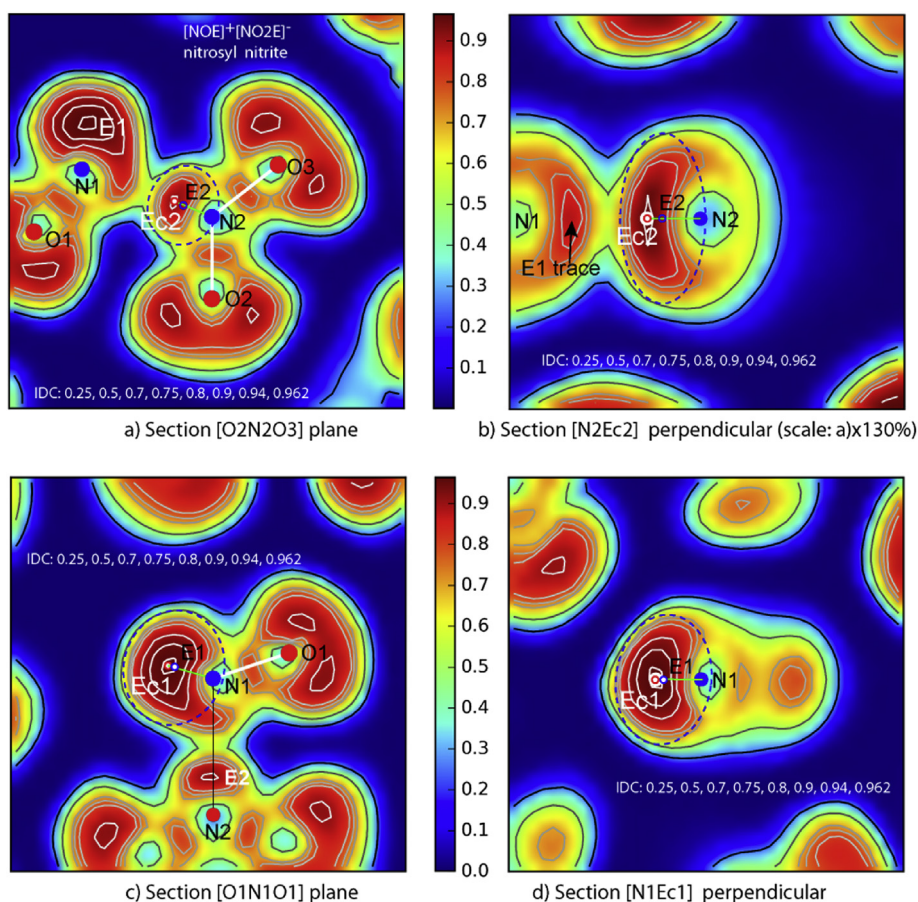


**Fig. 10.** ELF sections: a) Nitrite group plane N2O2O3; b) perpendicular plane to a) passing via N2-E2; c) nitrosyl group N1O1 + N2, d) perpendicular plane passing via N-E1.

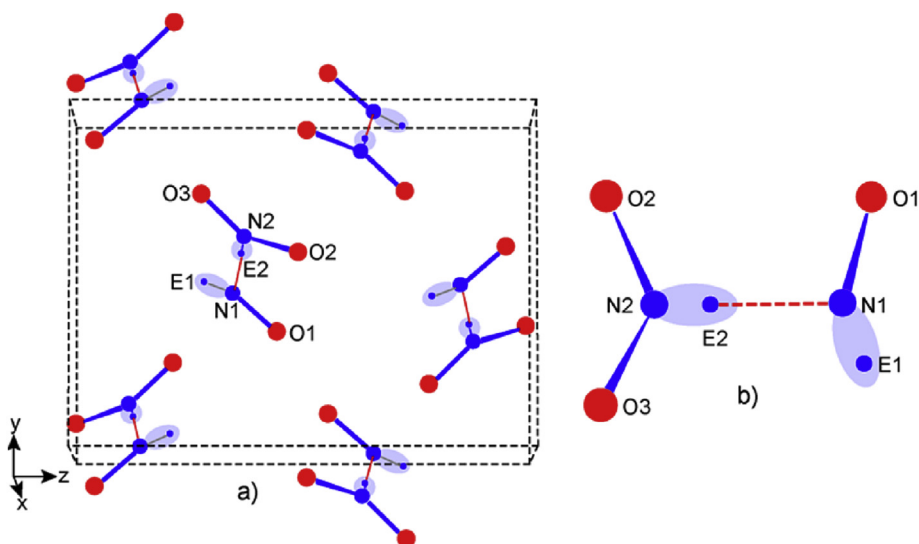


**Fig. 11.** Perspective views: a) orthonormal  $\text{N}_2\text{O}_3\text{E}_2$  network; b)  $[\text{NOE}]^+[\text{NO}_2\text{E}]^-$  nitrosyl nitrite molecule (dotted red stick indicates the ionic interaction N1 to Ec2 which firmly associate nitrite triangular unit and angular nitrosyl one).

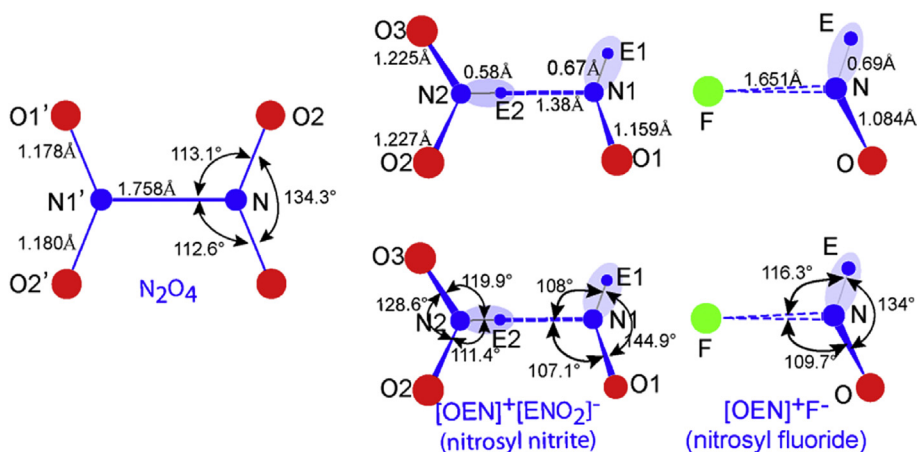


Fig. 12. Comparison of  $N_2O_4$ ,  $[E1O1N1-E2N2O2]$  and  $[EON-F]$  molecules (ELF data).

Table 4

$AgNO_2E$  crystal data [17] and DFT data.

$AgNO_2E$ – Orthorhombic, space group $Im\bar{m}2$ (No. 44).						
$a$ (Å)	$b$ (Å)	$c$ (Å)	$V$ (Å <sup>3</sup> )	$Z$	$V(Ag,O,E)$ (Å <sup>3</sup> )	
3.528	6.171	5.17	112.56	2	14.1	
3.613	6.452	5.122	119.4	2	14.9	
<b>Interatomic distances (Å) and angles (°)</b>						
N–O	1.154	N–Ag	2.471	Ag–Oef	2.425	
O–O	2.074	Ag–O	3.153	$\angle ONO$	127.9	
N–Oabcd	3.410	Ag–Oabcd	2.732	$\angle OeAgOf$	50.6	
N–E	0.61	Ag–E	1.861	E–Oabcd	3.077	
<b>Data from DFT-ELF analyses</b>						
N–Ec	0.62	N–Ag	2.240	Ec–Oabcd	3.084	
N–E	0.57	Ag–Ec	1.620	$r_E$	0.68	
N–O	1.266	Ag–Oef	2.449	Ec–E	0.13	
O–O	2.137	Ag–Oabcd	2.837	$\angle ONO$	115.1	
N–Oabcd	3.385	Ag–O	3.108	$\angle OeAgOf$	51.7	

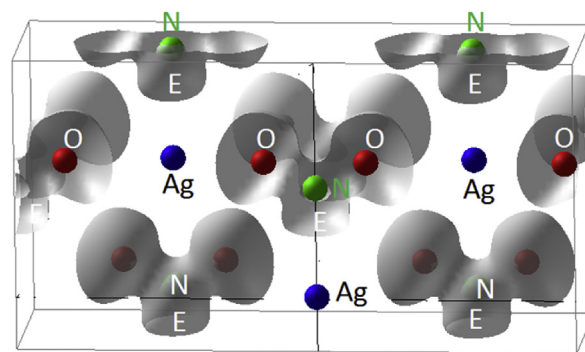


Fig. 14.  $AgNO_2$ . Calculated 3D ELF isosurfaces reproducing the schematic view in Fig. 13.

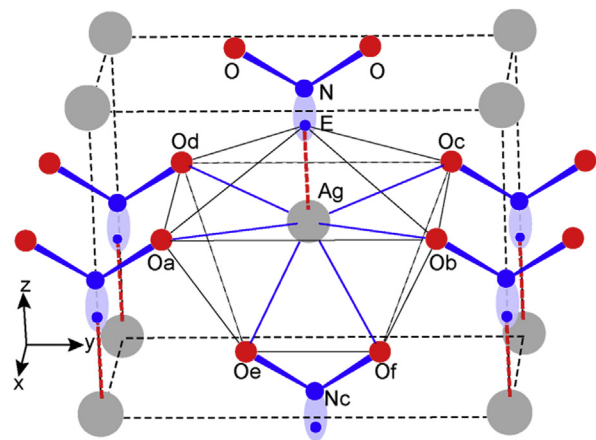


Fig. 13. Perspective view of  $AgNO_2E$  crystal structure.

including N–E in order to appreciate E extension in the [100] direction (Fig. 15).

DFT data show that  $a$  and  $b$  cell parameters are slightly bigger while  $c$  is shorter than for X-ray crystal data. Therefore if Ag–Oef and Ag–Oabcd distances are similar, the distance N–Ag is shorter. E is clearly evidenced in

Fig. 15a and b with a density maximum attributed to LP centroid Ec. N–Ec = 0.62 Å and the generated electron cloud is centered in E at ~0.13 Å from Ec. Between Ag and Ec, an ionic interaction is established, fixing  $NO_2^-$  on the top of the octahedron (Oef)OabcdE. This bonding shows that Ag–Ec = 1.620 Å and Ec–N = 0.62 Å, corresponding to the distance Ag–N = 2.24 Å. This scheme recalls the one in  $N_2O_3E_2$  even if the distances are bigger.

From these sections an E volume, approximated as an ellipsoid, was evaluated with  $a = 0.66$  Å,  $b = 0.44$  Å, and  $c = 1.06$  Å, grossly corresponding to a sphere of influence  $r_E = 0.68$  Å, a value close to the one of E2 in  $N_2O_3E_2$ , i.e.  $r_{E2} = 0.66$  Å.

## 7. $NCl_3E$

$NCl_3$  is an oily liquid at room temperature, with a yellow color. It crystallizes at low temperature below 233 K. X-ray data have been collected at 148 K as reported in Table 4 [18].

### 7.1. Crystal structure

The  $NCl_3$  crystal network contains three independent  $NCl_3E$  molecules which are organized in separated layers

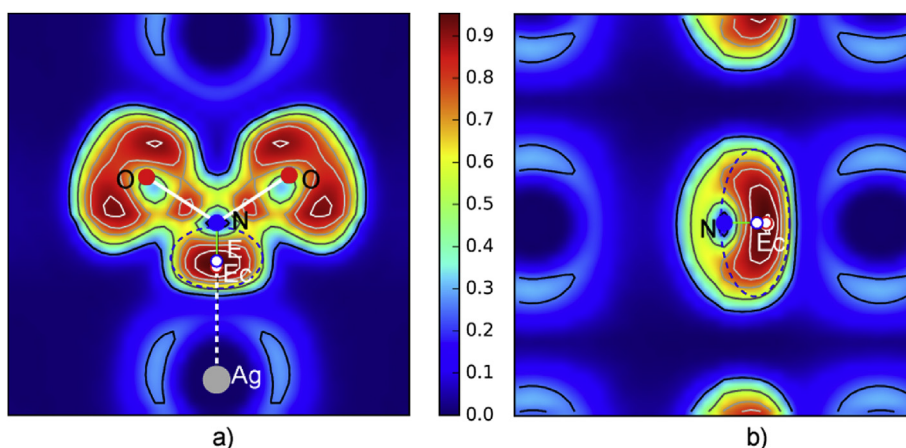


**Fig. 15.** ELF sections: a) section plane containing N, O and silver atoms showing the whole nitrite group with its lone pair E; b) the perpendicular plane passing through N–E.

parallel to the (010) plane centered onto mirror planes in  $y = 1/4$  and  $3/4$  as shown in Fig 16a (projection along [001]). Their thickness amounts to  $\Delta L = 2.813 \text{ \AA}$ ; the empty space slab showing a  $\Delta i = 0.185 \text{ \AA}$  value. To make a clear drawing of these layers, the one lying along the mirror in  $y = 1/4$  has been isolated; it is reported in Fig. 16b. The three molecules  $\text{N1Cl}_3$ ,  $\text{N2Cl}_3$  and  $\text{N3Cl}_3$  show a triangular prismatic shape. Then they have the classical  $\text{NCl}_3\text{E}$  tetrahedral geometry with their lone pairs opposite their one sided coordination to chlorine atoms. All of them exhibit very similar N–Cl bonds which evolve between  $1.712 \text{ \AA}$  and  $1.786 \text{ \AA}$  (see Table 4). The molecules  $\text{N1Cl}_3\text{E}$  and  $\text{N2Cl}_3\text{E}$  appear more condensed via large interactions (dotted lines values evolving from  $3.190 \text{ \AA}$  up to  $3.917 \text{ \AA}$ ) in the first half part of the cell along [001].  $\text{N3Cl}_3\text{E}$  molecules assume their interconnection and therefore the stability of the network. It is important to note the chlorine encapsulation of  $\text{N1E1}$ ,

$\text{N2E2}$  and  $\text{N3E3}$ , the former showing a  $[\text{N1E1}]\text{Cl}_6$  octahedron, the next two  $[\text{N2E2}]\text{Cl}_6$  and  $[\text{N3E3}]\text{Cl}_6$  being in triangular prisms more or less distorted. In our search for lone pair size, position and influence of the  $2s^2$  lone pair in this nitrogen trichloride was an interesting prototype to enrich our examples (see Table 5).

## 7.2. ELF calculation

After DFT-ELF calculations, pertinent parameters are shown in Table 4.

Fig. 17 shows the 3D ELF isosurface of  $\text{NCl}_3$ . The projection is presented at high isosurface value of  $0.881$  for the sake of clarity due to the large number of atoms in the unit cell. E on top of N is clearly shown. At such a high isosurface value, the ELF around Cl is observed as a torus enclosing the non bonded Cl electrons.

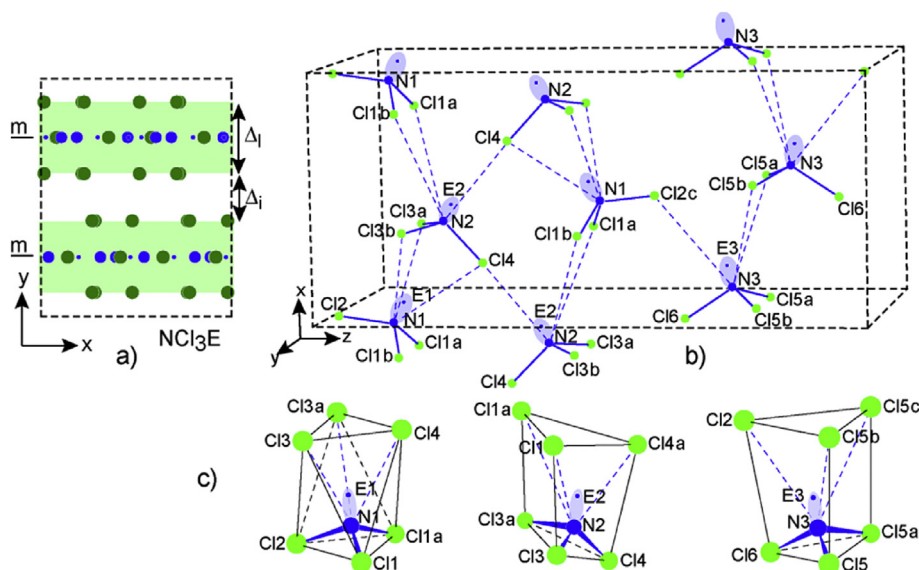


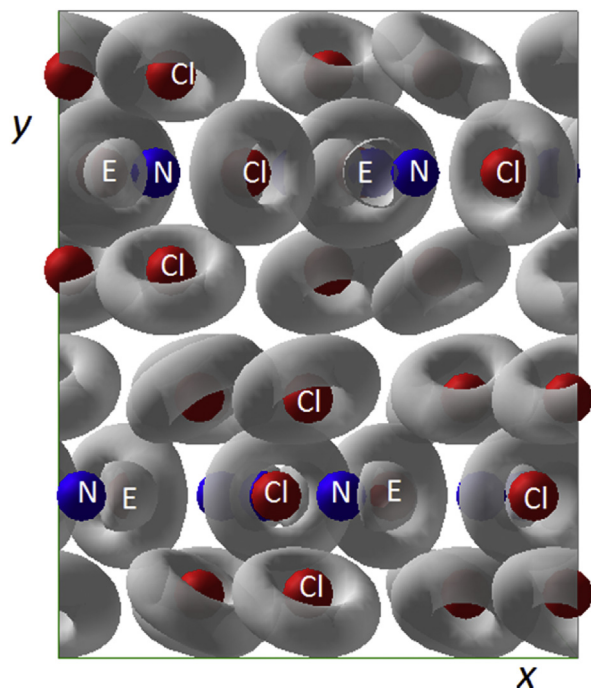
**Fig. 16.** a) View along [001] of the  $\text{NCl}_3$  network; b) perspective view of the layer parallel to the (010) plane formed by  $\text{NCl}_3\text{E}$  molecules and their interactions (dotted blue sticks); c) Coordination chlorine polyhedra around each independent  $[\text{N1E1}]$ ,  $[\text{N2E2}]$  and  $[\text{N3E3}]$ .



**Table 5**NCl<sub>3</sub>E crystal and DFT data [18].

<b>NCl<sub>3</sub>E</b> – Orthorhombic, space group <i>Pnma</i> (No. 62), <i>T</i> = 148 K						
<i>a</i> (Å)	<i>b</i> (Å)	<i>c</i> (Å)	<i>V</i> (Å <sup>3</sup> )	<i>Z</i>	<i>V</i> (Cl,E) (Å <sup>3</sup> )	
7.48	9.35	16.48	1152.6	12	24	
7.609	9.480	16.699	1204.6	12	25.1	
<b>Interatomic distances (Å) and angles (°)</b>						
N1–Cl1	1.731	N2–Cl3	1.786	N3–Cl5	1.786	∠Cl1a,bN1Cl2 107.4
a,b	a,b	a,b	a,b	a,b	a,b	
N1–Cl2	1.772	N2–Cl4	1.712	N3–Cl6	1.712	∠Cl1aN1Cl1b 109.5
N1–Cl3	3.298	N2–Cl1	3.917	N3–Cl5	3.685	∠Cl3a,bN2Cl4 108.1
a,b	a,b	a,b	a,b	a,b	a,b	
N1–Cl4	3.360	N2–Cl4a	3.190	N3–Cl2c	3.631	∠Cl3aN2Cl3b 105.2
						∠Cl5a,bN3Cl6 108.5
N1–E1	0.70	N2–E2	0.67	N3–E3	0.69	∠Cl5aN3Cl5b 104.8
E1–Cl3a, 3b	2.70	E2–Cl1a, 1b	3.48	E3–Cl5a, 5b	3.12	
E1–Cl4	2.79	E2–Cl4	2.56	E3–Cl2	3.07	
<b>Data from DFT-ELF analyses</b>						
N1–Ec1	0.68	N2–Ec2	0.70	N3–Ec3	0.68	
N1–E1	0.55	N2–E2	0.57	N3–E3	0.61	
N1–Cl1a,b	1.778	N2–Cl3a,b	1.783	N3–Cl5a,b	1.781	
N1–Cl2	1.779	N2–Cl4	1.782	N3–Cl6	1.808	
<i>r</i> <sub>E1</sub>	0.73	<i>r</i> <sub>E2</sub>	0.76	<i>r</i> <sub>E3</sub>	0.75	
∠Cl1a,bN1Cl2	107.9	∠Cl3a,bN2Cl4	107.7	∠Cl5a,bN3Cl6	107.3	
∠Cl1aN1Cl1b	107.4	∠Cl3aN2Cl3b	107.1	∠Cl5aN3Cl5b	106.3	

Then sections with iso-density curves throughout ELF data were performed right in the mirror plane of each molecule. They are illustrated in Fig. 18. Visibly they show that the three NCl<sub>3</sub>E molecules are quasi-identical. Therefore they were precisely analyzed in order to determine the position of the lone pair E and eventually if a maximum was detectable to show its maximal density concentration

**Fig. 17.** NCl<sub>3</sub>: 3D ELF view along xOy in a similar fashion to that in Fig. 16a.

(reasonably its centroid Ec), the N–Ec distance and assuming an ellipsoid shape, its two parameters *a* and *b* in the mirror, the third being determined in Fig. 18b,d,f the perpendicular sections to N–Ec.

N–Ec distances were readily measured as well as N–Cl ones allowing to determine the crystallographic coordinate of Ec. Then ellipses surrounding the electronic density [N–Ec] were made around each molecule giving the following *a/b/c* parameters: 0.79/0.67/0.75 Å for [N1–Ec1], 0.81/0.69/0.78 Å for [N2–Ec2] and 0.81/0.68/0.77 Å for [N3–Ec3]. Roughly, they correspond to lone pair spheres of influence with *r*<sub>E1</sub> = 0.73 Å, *r*<sub>E2</sub> = 0.76 Å and *r*<sub>E3</sub> = 0.75 Å. E centers of the ellipsoids, like in the other examples, are slightly off centered from the centroid Ec of lone pair, their large volume showing a less electronic density than the centroid Ec, rather well condensed, are more sensitive to the various repulsions of the network surroundings. Therefore it is worth noting the small distance between Ec and E ~0.12 Å.

From these experiments, an average distance N–Cl = 2.10 Å to chlorine atoms of triangular prismatic NCl<sub>3</sub> molecule base has been extracted and transferred to crystal data to localize E1, E2 and E3 lone pairs by using their coordinates. To control that, their volumes of influence are well set up in [NE] coordination polyhedra, and distances with remaining chlorines were calculated. They show an average value of 3.00 Å, much higher than E–Cl = 2.10 Å, making this insertion acceptable (Table 4).

Therefore, data of the NCl<sub>3</sub>E crystal structure have been completed (blue printed values) favoring a full understanding of its atomic architecture, the molecules being put together to build layers [NCl<sub>3</sub>E]<sub>n</sub> by a cobweb of long N–Cl weak bonds. The layers packed along [010] are held by Van der Waals interactions.

## 8. Conclusion

This work was devoted to the formal 2s<sup>2</sup> lone pair (LP) behavior in simple fundamental molecules. The aim was to find LP position, to evaluate its “volume of influence” which consists in an electron cloud generated around the centroid Ec of the electronic doublet. We considered basic molecules formed around nitrogen atom: NH<sub>3</sub>E ammonia, [NOE]<sup>+</sup>F<sup>−</sup> the nitrosyl fluoride, [NOE]<sup>+</sup>[NO<sub>2</sub>E]<sup>−</sup> nitrosyl nitrite (plus AgNO<sub>2</sub>E silver nitrite) and NCl<sub>3</sub>E nitrogen trichloride.

Like in our approach of these problems with the 6s<sup>2</sup> elements (Tl, Pb, Bi, Po), the LP role in the crystal network architecture is of paramount importance [1–3,5,6]. Using new analytic software, it has been possible to complete electron localization function (ELF/DFT) calculations by making precise sections within three dimensional electron localization which allowed setting up Ec, a small volume of maximum intensity in an E electron cloud.

Ec position was then determined, cloud volume and its center E always with a position slightly distinct from Ec (~0.12 ± 0.02 Å) and closer to N. The size of the lone pair in all these compounds does not show strong differences: *r*<sub>ENH<sub>3</sub></sub> = 0.65 Å, *r*<sub>EAgNO<sub>2</sub></sub> = 0.77 Å and 0.66 Å, *r*<sub>EAgNO<sub>2</sub></sub> = 0.68 Å, *r*<sub>ENOF</sub> = 0.78 Å and *r*<sub>EN<sub>1</sub>Cl<sub>3</sub></sub> = 0.73 Å, *r*<sub>EN<sub>2</sub>Cl<sub>3</sub></sub> = 0.76 Å, and *r*<sub>EN<sub>3</sub>Cl<sub>3</sub></sub> = 0.75 Å.



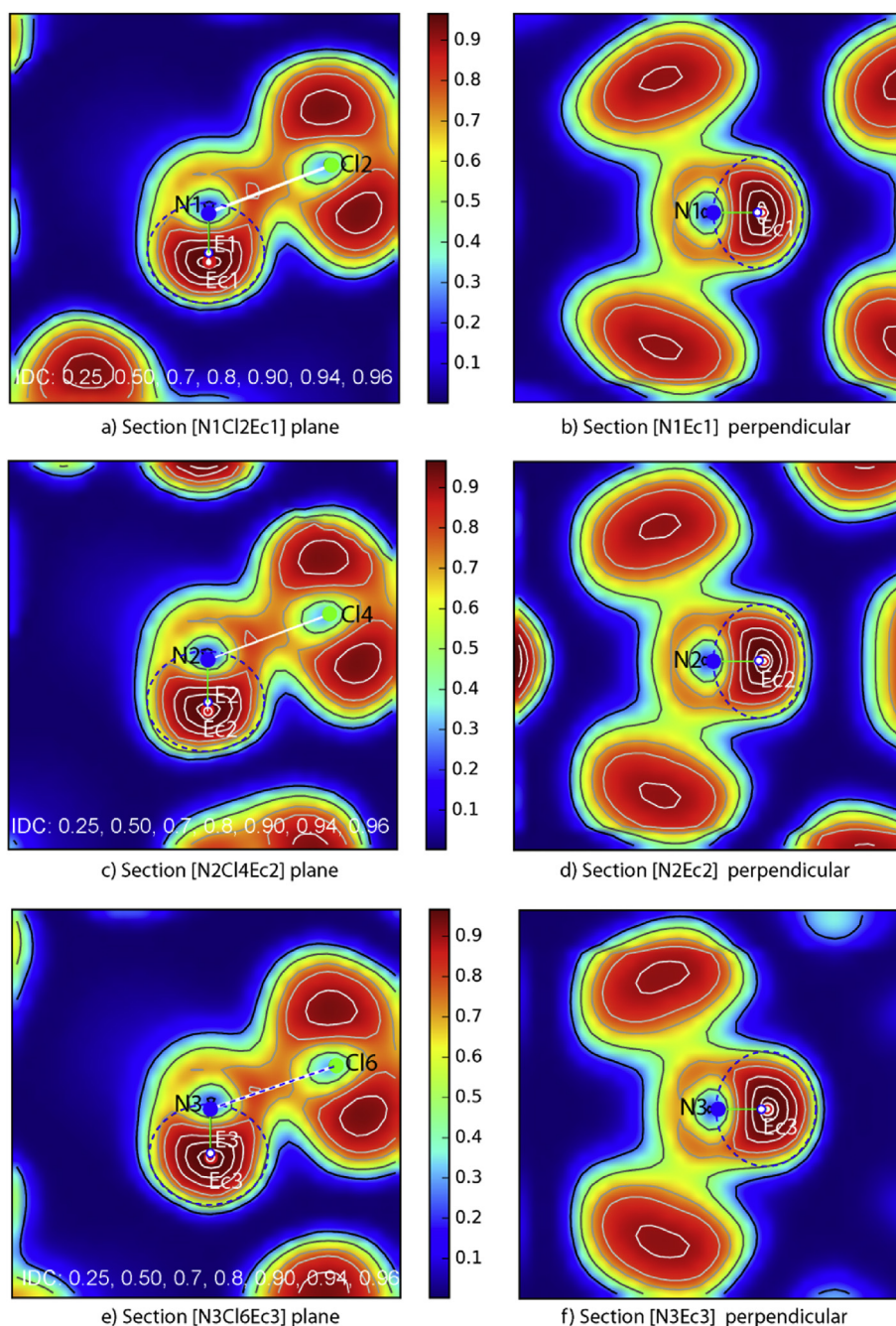


**Fig. 18.** ELF sections: a,c,e) planar sections containing N, Cl and E atoms in the mirror plane of the three independent molecules N1, N2 and N3; b,d,f) the perpendicular plane to N–Ec in Ec for each molecule.

The determination of the E2 lone pair position in the nitrite group  $[\text{N1OE1}]^+[\text{N2O}_2\text{E2}]^-$  of nitrosyl nitrite has evidenced a strong ionic N1–E2 interaction, allowing to understand the stability of the whole molecule even during its crystal structure phase transition, a linear sequence N2–Ec2–N being substituted to the “extraordinary long N2–N1 bond (1.890 Å)”. This direct ionic interaction with lone pair centroid was unexpected; therefore, an analogous situation occurs in  $\text{AgNO}_2\text{E}$ , silver nitrite, where Ag is directly online with E of nitrite group.

## 9. Short annex on the theory framework

It is now established in quantum physics and chemistry that an accurate way to account for exchange and correlation (XC) albeit at the local level, is carried out within the density functional theory (DFT) [7,8]. The first account of XC effects was first approximated with the local density approximation (LDA) [19] scheme based on the homogeneous electron gas. However introducing gradients to the electron density was rapidly needed with the GGA

(generalized gradient approximation, used in the present work [20]). The subsequent success of the DFT, in accounting for the physical properties of a broad panel of compounds, led to building many methods around it with different levels of outcomes of electronic and magnetic band structures, chemical bonding properties and other energy related properties as mechanical ones (enthalpies, bulk modules, elastic constants, etc.).

In our work we used the Vienna ab initio simulation package (VASP) code [21,22] to obtain equilibrium crystal structures which are actually close to experimental determination. The purpose is here to subsequently 'build' the electron localization around the chemical constituents: i.e. the atoms with their chemical trend to ionization either positively—decrease of localization—or negatively—increase of localization. This can be done through different schemes such as the electron localization indicator (ELI-D) [23] or the electron localization function (ELF) used here [9]. The ELF scheme is based on the kinetic energy in which the Pauli Exclusion Principle is included:  $ELF = (1 + \chi_\sigma^2)^{-1}$  with  $0 \leq ELF \leq 1$ , i.e. it is a normalized function. In this expression, the ratio  $\chi_\sigma = D_\sigma/D_\sigma^0$ , where  $D_\sigma = \tau_\sigma - \nabla s - \frac{1}{4}(\nabla \rho_\sigma)^2/\rho_\sigma$  and  $D_\sigma^0 = 3/5 (6\pi^2)^{2/3} \rho_\sigma^{5/3}$  correspond, respectively, to a measure of Pauli repulsion ( $D_\sigma$ ) of the actual system and to the free electron gas repulsion ( $D_\sigma^0$ ) and  $\tau_\sigma$  is the kinetic energy density. Then a normalization of the ELF function between 0 (zero localization) and 1 (strong localization) with the value of  $\frac{1}{2}$  corresponding to a free electron gas behavior enables analyzing the contour plots following a color code: blue zones for zero localization, red zones for full localization and green zone for  $ELF = \frac{1}{2}$ , corresponding to a free electron gas. Besides the 2D ELF representation we mainly consider the 3D iso-surfaces enclosing the electrons of each atomic constituent. This paper shows the usefulness of such 3D representations for the discussion of the lone pair development and stereo-activity.

## Acknowledgements

Computations were conducted at the MCIA-University of Bordeaux computer centre. JG thanks Pra. Alicia Castro for fruitful scientific partnership between LCTS and ICMC.

Support from CNRS and CSIC is gratefully acknowledged.

## References

- [1] R.J. Gillespie, R.S. Nyholm, Q. Rev. Chem. Soc. 11 (1957) 339.
- [2] R.J. Gillespie, I. Hargittai, The VSEPR Model of Molecular Geometry, Allyn and Bacon, 1991, p. 149.
- [3] S. Andersson, A. Aström, Solid State Chemistry, in: Proc. 5th Material Research Symposium, 364, NBS Special Publication, 1972, pp. 3–13.
- [4] J. Galy, G. Meunier, S. Andersson, A. Aström, J. Solid State Chem. 13 (1975) 142.
- [5] S.F. Matar, J. Galy, Prog. Solid State Chem. 43 (2015) 82–97, <http://dx.doi.org/10.1016/j.progsolidstchem.2015.05.001>.
- [6] J. Galy, S.F. Matar, Prog. Solid State Chem. 44 (2016) 35–58 (account).
- [7] P. Hohenberg, W. Kohn, Phys. Rev. B 136 (1964) 864.
- [8] W. Kohn, L.J. Sham, Phys. Rev. A 140 (1965) 1133.
- [9] A.D. Becke, K.E. Edgecombe, J. Chem. Phys. 92 (1990) 5397; Nature, 371 (1994) 683.
- [10] H. Mark, E. Pohland, Z. Kristallogr. 62 (1925) 103.
- [11] R. Boese, N. Niederpruem, D. Blaese, A.H. Maulitz, M.Y. Antipin, P.R. Mallinson, J. Phys. Chem. 101 (1997) 5794–5799.
- [12] E. Vila, Lone pair coordinates calculation in solid state crystal structures, private communication, ICMC/CSIC, Madrid, Spain.
- [13] G. Couégnat, unpublished results, 2015.
- [14] A. Ellern, K. Seppelt, Z. Anorg. Allg. Chem. 627 (2001) 234–237.
- [15] J. Horak, H. Borrmann, A. Simon, Chem. Eur. J. 1 (6) (1995) 389–393.
- [16] A. Obermeyer, H. Borrmann, A. Simon, Z. Kristallogr. 196 (1991) 129–135.
- [17] R.E. Long, R.E. Marsh, Acta Crystallogr. 15 (1962) 448–450.
- [18] H. Hartl, J. Schoener, J. Jander, H. Schulz, Z. Anorg. Allg. Chem. 413 (1975) 61–71.
- [19] D.M. Ceperley, B.J. Alder, Phys. Rev. Lett. 45 (1980) 566.
- [20] J. Perdew, K. Burke, M. Ernzerhof, Phys. Rev. Lett. 77 (1996) 3865.
- [21] G. Kresse, J. Furthmüller, Phys. Rev. B 54 (1996) 11169.
- [22] G. Kresse, J. Joubert, Phys. Rev. B 59 (1999) 1758.
- [23] F.R. Wagner, V. Bezugly, M. Kohout, Y. Grin, Chem. Eur. J. 13 (2007) 5724.